

Mold Design, Fabrication and Tensile Testing
of EMBED-812, a Tissue Embedding Epoxy Resin

by

Lucy W. Du

Massachusetts Institute of Technology, 2014

Submitted to the Department of Mechanical Engineering
in Partial Fulfillment of the Requirements for the Degree of
Bachelor of Science in Mechanical Engineering

at the

Massachusetts Institute of Technology

June 2014

© 2014 Massachusetts Institute of Technology
All rights reserved.

Signature of Author.....
Department of Mechanical Engineering
15 May 2014

Certified by.....
Martin L. Culpepper
Professor of Mechanical Engineering
Thesis Supervisor

Accepted by.....
Annette Hosoi
Associate Professor of Mechanical Engineering
Undergraduate Officer

Mold Design, Fabrication and Tensile Testing
of EMBED-812, a Tissue Embedding Epoxy Resin

by

Lucy W. Du

Submitted to the Department of Mechanical Engineering
on May 15, 2014 in Partial Fulfillment of the
Requirements for the Degree of Bachelor of Science in
Mechanical Engineering

ABSTRACT

Serial sectioning is a process whereby fixed tissue is embedded in a polymer to preserve structure and is then sliced into very thin sections as small as 25nm. Currently, there is a lack of understanding of this embedding material, preventing accurate and clean slicing at this level of precision. This thesis focuses on performing tensile tests to determine some of the material properties—elastic modulus, ultimate tensile strength, yield strength—of the epoxy resin used to embed fixed brain tissue. These results will be used in cutting models and help guide the development of a next-generation cutting instrument for automated serial sectioning of tissue. Ultimately, this machine will make it possible to section and image large volumes of brain tissue, leading to further understanding of neural activity and mechanisms behind cognition and tissue disease. This understanding will make it possible to develop treatments for currently untreatable neural diseases and disorders. This research involves creating a streamlined tensile testing procedure for the embedding epoxy resin, EMBED-812, as well as the analysis of tensile tests. The elastic modulus, ultimate tensile strength, yield strength, and percent elongation at break of EMBED-812 were found to be 4.24 ± 0.27 GPa, 44.8 ± 4.0 MPa, 17.2 ± 2.6 MPa, and $3.73 \pm 1.27\%$, respectively. This testing process can be improved and further work is suggested.

Thesis Supervisor: Martin L. Culpepper
Title: Professor of Mechanical Engineering

ACKNOWLEDGEMENTS

I would like to thank Prof. Martin Culpepper for the amazing opportunities he has given me while working in his lab during my undergrad at MIT. I have learned so much about research and engineering during this time, and I look forward to learning even more while earning my graduate degree. I would also like to thank Aaron Ramirez for guiding me throughout this whole thesis process, and bearing with me through long machining days; you were so busy with your own work, but still somehow found time to patiently sit with me time after time to help me proceed through roadblock after roadblock on my thesis. Next, there is Marcel Thomas, who I somehow convinced to come help me machine for a whole day on a weekend. Thanks for all the advice about machining, research, thesis writing, and life at MIT in general. I would also like to thank Pierce Hayward for the tensile testing guidance.

Last but not least, I would like to thank Julie Wang and Rachel Dias Carlson, my fellow bachelor thesis-ers, along with my other friends, who, over the course of this last semester, heard nothing but endless woes, complaints, victory and defeat stories about my thesis. You have helped motivate and encourage me through all the setbacks and moments of panic over graduation. Thanks for putting up with me!

CONTENTS

Abstract.....	3
Acknowledgements	5
Contents	7
Figures.....	9
Tables	10
1 Introduction.....	11
1.1 Background on Ultramicrotomy	12
1.1.1 Ultramicrotomy Processes and Procedure.....	12
1.1.2 Current Ultramicrotomes.....	15
1.1.3 Limitations	17
1.2 Background on Embedded Tissue	18
1.2.1 Embedding Techniques.....	18
1.2.2 Epoxy Material Properties.....	18
1.3 Background on Cutting Models.....	19
1.3.1 Williams Model.....	19
1.3.2 Wyeth-Atkins Model.....	20
1.4 Thesis Structure	21
2 Material Property Calculations.....	23
2.1 Elastic Modulus	23
2.2 Ultimate Tensile Strength	24
2.3 Yield Strength.....	24
3 Experimental Design.....	27
3.1 Test Overview.....	27
3.2 Mold Design.....	28
3.2.1 Mold Fabrication.....	33

3.3	Specimen Preparation	33
3.4	Experimental Design.....	36
3.5	Sources of Error	37
4	Results	39
4.1	Experimental Results	39
4.2	Discussion.....	41
5	Conclusion	43
5.1	Summary.....	43
5.2	Future Work.....	44
5.2.1	Mold Improvements	44
5.2.2	Further Materials Testing.....	44
	References.....	46
A	Mold Design and Fabrication.....	47
A.1	Mold CAD Drawings.....	47
A.2	Calculations.....	48
A.2.1	Separation Force Calculations.....	48
A.2.2	Deflection Calculations	49
A.3	Mold Centerpiece Process Plans.....	50
B	Specimen Production	53
B.1	Actual Specimen Mixture Quantities.....	53
B.2	Actual Specimen Dimensions	53
C	Individual Specimen Material Property Values.....	55

FIGURES

Figure 1.1: Ultramicrotomy Process.....	14
Figure 1.2: State of the art sectioning machines.	16
Figure 3.1: Tensile test specimen diagram and dimensions [11]......	28
Figure 3.2: Mold design concept comparison.	30
Figure 3.3: CAD model of the assembled mold.	31
Figure 3.4: Epoxy mixing and specimen preparation procedure.	35
Figure 3.5: Specimen setup in the Instron with extensometer.	36
Figure 4.1: Annotated stress-strain curve for Specimen 7.....	40
Figure 4.2: Stress-strain curves for all eight test specimens.	41
Figure A.1: Dimensioned drawing of mold centerpiece.....	47
Figure A.2: Maximum separation force calculations.....	48
Figure A.3: Average separation force calculations.....	49
Figure A.4: Mold deflection calculations.	49
Figure A.5: Mold centerpiece process plan used for this thesis.	51
Figure B.1: Labeled schematic of relevant testing specimen dimensions.	53

TABLES

Table 1.1: Summary of EMBED-812 material properties.....	11
Table 1.2: State-of-the-art sectioning machine comparison.	17
Table 1.3: Williams model cutting regimes [9].	20
Table 3.1: Mold functional requirements.....	29
Table 3.2: EMBED-812 mixing ratios.	34
Table 4.1: EMBED-812 material property values.....	41
Table B.1: Actual quantities in epoxy mixtures.....	53
Table B.2: Measured dimensions of molded specimens in mm.	54
Table C.1: Material property values for each separate specimen.	55

INTRODUCTION

Serial sectioning is a process whereby a tissue is embedded in a polymer to preserve structure and is then sliced into very thin pieces as small as 25nm. The purpose of this research is to understand the some of the material properties—elastic modulus, ultimate tensile strength, Poisson’s ratio—of the epoxy resin used to embed fixed brain tissue. It is important to understand the material properties of these materials in order to determine the cutting mechanisms required to cut these materials at the nanoscale. The results from this thesis will be used to determine the feasibility of cutting these materials at such a small scale as well as guide the development of a next-generation cutting instrument for automated serial sectioning of tissue. Ultimately, the machine will make it possible to section and image large volumes of brain tissue, leading to further understanding of neural activity and mechanisms behind cognition and tissue disease. This understanding will make it possible to develop treatments for currently untreatable neural diseases and disorders.

The material properties calculated from the data collected in this thesis are shown below in Table 1.1 below.

Table 1.1: Summary of EMBED-812 material properties.

Material Property	Value
Elastic Modulus	4.24 ± 0.27 GPa
Ultimate Tensile Strength	44.8 ± 4.0 MPa
Yield Strength (0.2% offset)	17.2 ± 2.6 MPa
% Elongation at Break	3.73 ± 1.27 %

This research involves creating a streamlined tensile testing procedure for the embedding epoxy resin, EMBED-812, as well as the analysis of tensile tests. There are three general phases of this research: design and fabrication of the testing sample mold, molding the samples themselves, and tensile testing of the samples.

1.1 Background on Ultramicrotomy

Ultramicrotomy is a method for sectioning specimen, usually biological, into extremely thin slices that can then be viewed in a transmission electron microscope (TEM). This is generally a very difficult technique, requiring patience and practice. When TEMs were developed in the 1930s, they instantly became important tools for the structural analysis of biological objects. However, spatially extensive biological structures cannot be readily and easily be imaged using TEMs for a variety of reasons. The quality of images depends highly upon the thickness of the specimen, so tissue samples must be cut into thin slices before imaging, creating the need for ultramicrotomy. Another obstacle is the low contrast of biological tissues; in order to see the features, they have to be enhanced using staining compounds. Lastly, the use of the TEM means that the samples will be brought into a high vacuum; the biological materials need to be stabilized against collapse in this environment. Several methods of embedding chemically fixed tissue samples in various polymers were developed and improved over time. The embedded tissue would be mechanically stable in the vacuum and the electron beam while also making it easier for thin sectioning of the tissue samples [1].

1.1.1 Ultramicrotomy Processes and Procedure

Current ultramicrotomes are operated manually and sections are made by facing a specimen block—usually 1mm^3 or smaller—using a glass or diamond knife. Currently, small dehydrated and fixed tissue samples are molded into a long cylinder or prism. The tissue is usually embedded at one end of the cylinder or prism, as shown in Figure 1.1a. More details about embedding epoxies and processes are described later in Section 1.2. After the sample is removed from the mold, it is then placed in a specimen holder and, using a prep blade, excess plastic is shaved off, exposing the specimen in the block face. These preliminary sections are usually made at rather large thickness settings (800nm). The plastic on the sides of the sample is also typically cut away to form a trapezoidal shape at the end with the tissue specimen, as shown in Figure 1.1b. This is done because the smaller the trimmed block face, the easier thin sectioning will be [2].

For thick sections ($\sim 800\text{nm}$), wet glass knives with integral boats are used; for thinner sections, diamond knives or balanced-break glass knives attached to a boat with water are generally used. Figure 1.1c shows an image of a typical ultramicrotome knife with an attached

boat. After proper alignment and preparation of the blade, the water level should be adjusted using a micropipette, as shown in Figure 1.1d, and the ultramicrotome can begin to section the sample. As the knife slices through the specimen, the chip glides over the edge of the knife and is collected by the water in the boat (Figure 1.1e). Using the water-filled boat will minimize damage to the slice after it is cut off from the block. The slice can then be picked up from the boat using a micropipet and transferred to a glass slide for imaging using either a light microscope or a TEM (Figure 1.1h). For ultra-thin slices (40-150nm), slices are picked up using a copper EM grid [2].

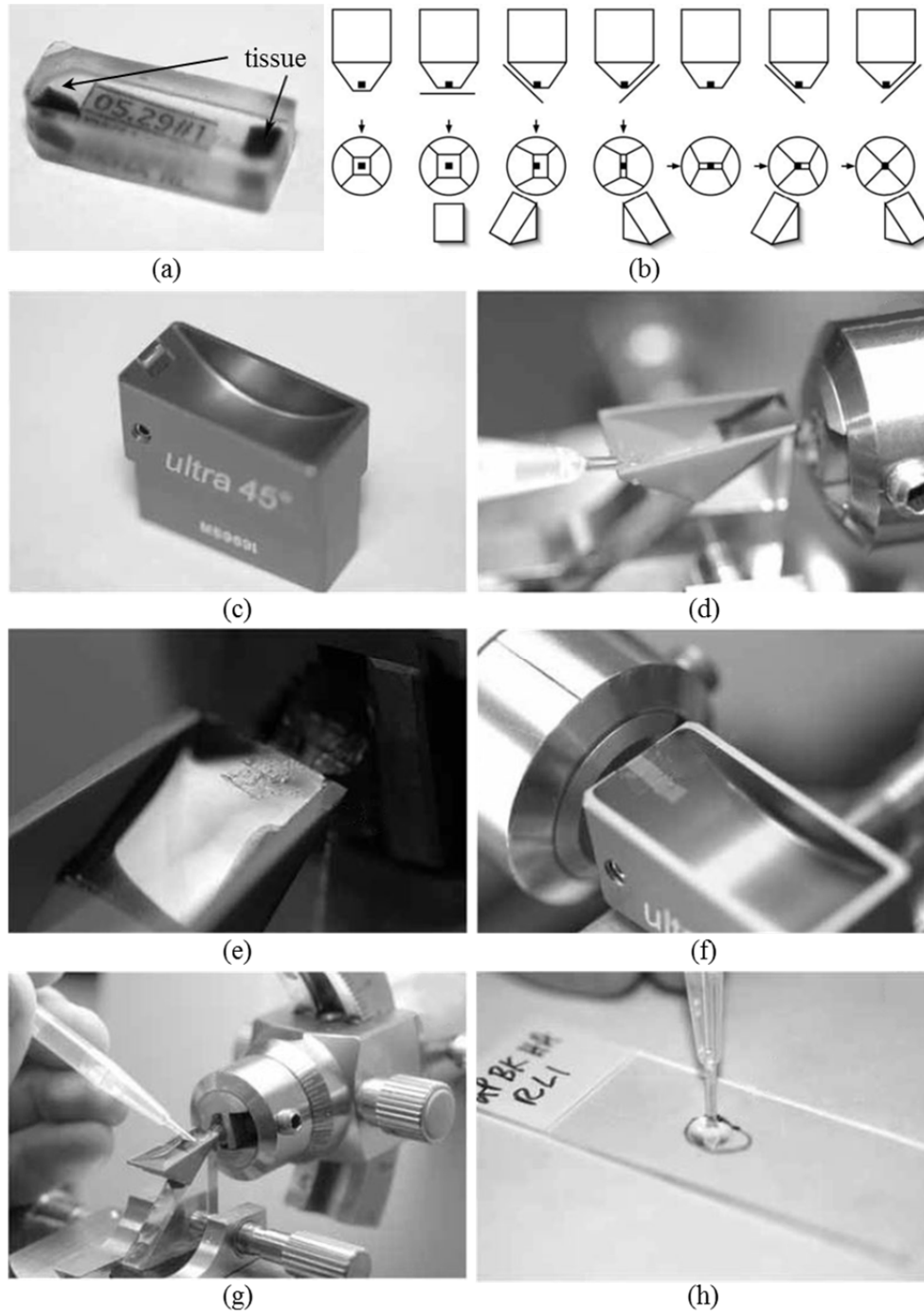


Figure 1.1: Ultramicrotomy Process¹

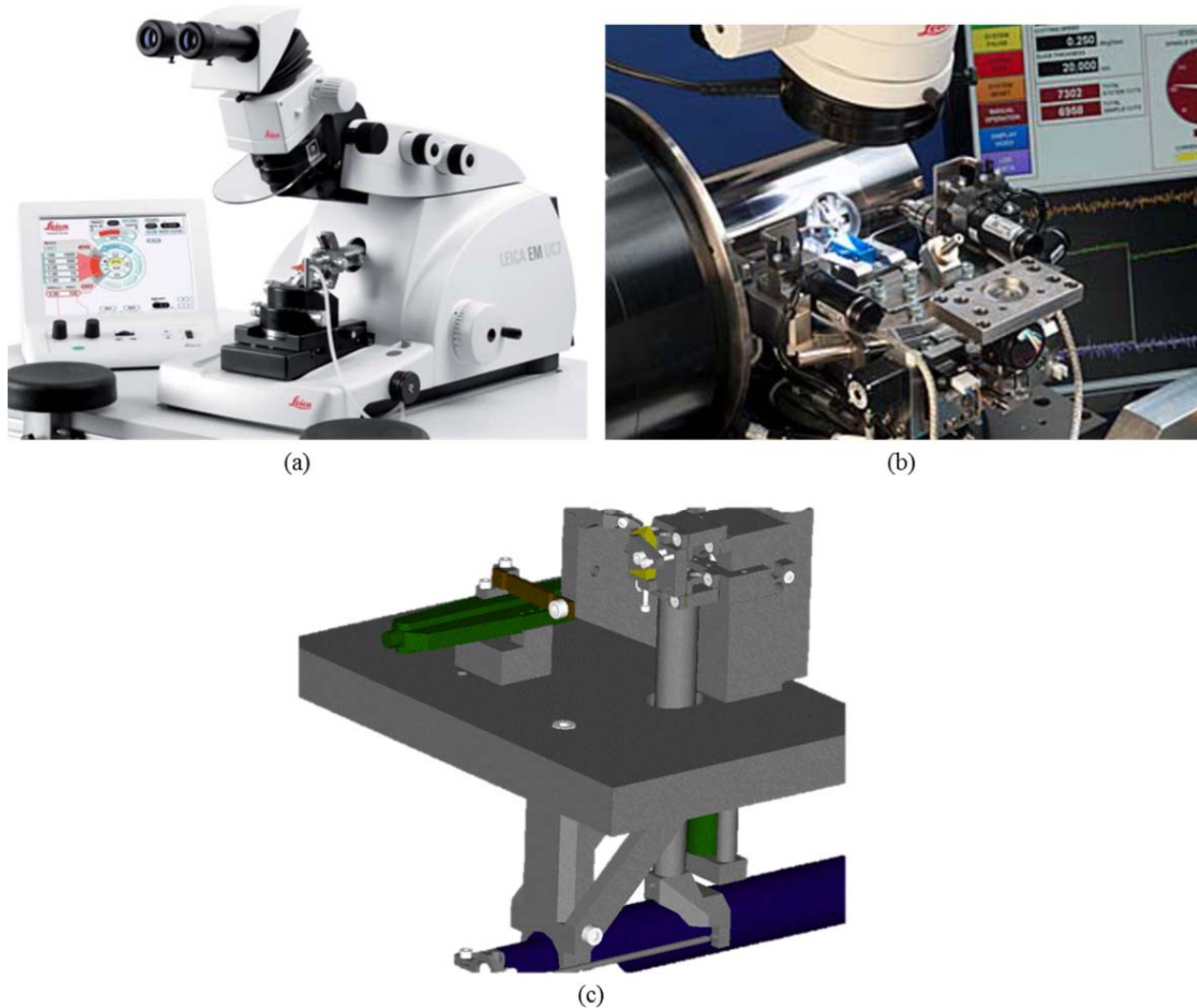
(a) An epoxy block with embedded tissue samples on each end. (b) Process for tapering a block for sectioning. (c) Close up of diamond knife and integral boat for water. (d) A micropipet adjusting water level in the boat. (e) Thick sections that are cut float adjacent to the knife edge ready to be picked up. (f) Thin sections. (g) A micropipet picking up floating thick sections and (h) transferring them to a slide for microscopy.

¹ Figure 1.1 reproduced with permission from Copyright Clearance Center. Copyright 2007 by Springer Science.

1.1.2 Current Ultramicrotomes

Currently, an ultramicrotome is used to section each individual slice, and a microtome would manually place each slice on a glass slide for TEM or light microscopy imaging. One state-of-the-art ultramicrotome commonly used is the Leica EM UC7 Ultramicrotome, shown in Figure 1.2a. The Leica EM UC7 is a standard ultramicrotome used in research labs designed to be ergonomic and intuitive for both highly skilled and beginner ultramicrotomists. It has a fully motorized knife stage and an automated trimming program, making the sample preparing steps of ultramicrotomy much easier and less tedious. The ultramicrotome also comes with a stereomicroscope so ultramicrotomists can observe the sectioning in real time [3]. With this standard ultramicrotome, the process is still manual, slow, and unpredictable. The process is only reliable and repeatable when performed by skilled technicians and researchers.

Recently, there have been other ultramicrotomes that have been developed into automated serial sectioning machines. One such machine is the Automatic Tape-collecting Lathe UltraMicrotome, or ATLUM for short, developed by Boston Engineering, see Figure 1.2b. The initial target specifications for this machine were to allow amateur researchers to reliably slice and collect tissue samples without damage at thicknesses as small as 20nm, as well as automating the slicing process, so at least 10,000 sections could be collected over time without operator intervention [4]. This machine took a new approach; instead of having the knife make separate sections, the machine essentially acts like a lathe and produces a continuous ribbon of tissue by turning an ultrathin strip off the surface of a cylindrical block of multiple tissue blocks. The knife stays engaged to the tissue block at all times, and the ribbon of tissue is fed into the water-boat of the knife to catch the continuous ribbon of tissue sections [5]. When tested, however, this machine did not perform up to the initial specifications. The slices were around 40nm, which are too large to get the imaging resolution required. Furthermore, ATLUM could only cut up to 400 sections without failure for slices at a thickness of 45nm. At a thickness of 38nm, the best test run only produced 295 sections [6]. In order for this machine to image a whole brain, the number of continuous sections must improve by at least two orders of magnitude. Though the machine was designed to be able to slice 20nm thin sections, there is no discussion about why this has not been achieved.



(a)

(b)

(c)

Figure 1.2: State of the art sectioning machines.

(a) Leica EM UC7 Ultramicrotome² (b) Automatic Tape-collecting Lathe UltraMicrotome (ATLUM)³ (c) Denk-Horstmann serial sectioner⁴.

One other recently developed serial sectioner is the Denk-Horstmann serial sectioner. This device uses Serial Block-Face Scanning Electron Microscopy (SBF-SEM), combining the sectioning and imaging. Unlike classic ultramicrotomes, this serial sectioner images the block-face itself rather than the removed sections. Using this method, the problem of automatically

² Figure 1.2a reproduced with permission from <<http://www.leica-microsystems.com>>. Copyright 2013 by Leica Mikrosysteme, GmbH, Vienna, Austria.

³ Figure 1.2b reproduced with permission from ASPE Publications. Copyright 2013 by ASPE.

⁴ Figure 1.2c reproduced with permission from PLOS through a Creative Commons Attribution license.

collecting the removed slices is no longer relevant. This serial sectioner is able to image hundreds of sections at a thickness of 50-70nm. Due to excessive chatter, thinner sections cannot be made. While this resolution is adequate for most cellular organelles and synaptic specializations, it is highly desirable to be able to reliably cut thinner sections—around 20-25nm [7].

1.1.3 Limitations

There are several limitations in existing processes of ultramicrotomy: (1) thickness (2) size (3) speed. As previously mentioned, current ultramicrotomes can only reliably produce slices at 40nm or thicker. This thickness is still too large to image some important features, such as vesicles and stained proteins. Furthermore, ultramicrotomes can only section small blocks of tissue that are fixed in the epoxy resin. When the surface area of the block increases, it becomes increasingly difficult to produce thin slices without defects. These specimen blocks are usually 1mm³ or smaller, which is significantly smaller than the volume of a mouse brain, let alone a human brain. With regards to speed, the current process of ultramicrotomy is almost entirely manual. With practice, the whole process of creating a slice and producing a slide takes about 15minutes. It takes at least a few weeks of practice to achieve this level of skill. If an entire mouse brain were to be imaged using this method, it would take about 10,000 hours for an ultramicrotome to slice and make slides of only a 1mm³ sample, assuming 25nm sections. This does not include any fixation time or imaging time [2].

Table 1.2: State-of-the-art sectioning machine comparison.

Parameter	Leica EM UC7	ATLUM	Denk-Horstmann
Slice Thickness	40-800 nm	~40 nm	~50 nm
# of serial sections	1	400	Hundreds
Automated	No	Yes	Yes

From Table 1.2, it is evident that, using existing technology, there is no way to automatically and continuously section large volumes of tissue at thicknesses of 25nm. The need of an automated serial sectioning machine that can reliably make cuts at this thickness would be a large technological step.

The ATLUM and Denk-Horstmann serial sectioner both have solutions to the issue of automated serial sectioning. Both of these devices face the issue that they cannot produce thin

enough slices. Given the current technology and knowledge, it is not possible to cut accurately at the nanoscale due to lack of understanding of the sectioning material properties and how they affect cutting. The work in this thesis provides the first step to shedding light on the material properties of the embedding material, which will in turn lead to more information on the cutting mechanisms and forces involved with ultramicrotomy.

1.2 Background on Embedded Tissue

Ultramicrotomy of biological materials requires living specimens to be transformed to a dry state that faithfully maintains the structural and biological relationships that the researcher is interested in studying [2]. A common way to preserve the structural and biological integrity of the tissue is to dehydrate and fix the tissue in an aldehyde and embed it in a polymer.

1.2.1 Embedding Techniques

Initially in conventional microtomy, waxes and paraffines were used for embedding specimens for thin sectioning. However in 1949, *n*-butyl methacrylate was introduced as an embedding resin. The hardness of this embedding resin could easily be varied, allowing researchers to adjust the material properties of the resin to match the cutting parameters they needed. In 1956, epoxies quickly became the leading method for embedding tissue. The most influential epoxy resin was “Epon 812,” an aliphatic epoxy resin introduced in 1959. Luft published major improvements in the embedding protocol for Epon 812, and it quickly became the leading epoxy resin used in ultramicrotomy. Since then, there have been other resins that have been developed—such as Durcupan—but the compound for Epon 812 still remains a commonly used embedding medium [1]. The manufacturer of Epon 812 has since discontinued production, but Electron Microscopy Sciences has created EMBED-812, a direct replacement with the same properties and preparation procedures as Epon 812. The procedure for epoxy preparation that Luft published in 1961 is still used today for EMBED-812.

1.2.2 Epoxy Material Properties

The current challenge in ultramicrotomy is the difficulty of reliably sectioning at a thickness of around 25nm. This challenge can be overcome by further understanding the cutting forces related to sectioning embedding media and tissue at the nanoscale. The first step to

understanding the cutting forces is to have a grasp on the material properties of the embedding medium. Acetarin *et al.* [8] have previously investigated some related mechanical properties of various embedding resins by performing tensile, compression, flexibility, and hardness tests following the respective standards. Epon 812 was one of the embedding resins that were tested in this series of experiments, and the results of various material properties were then compared against a qualitative scale of cutting grade [8].

These experiments were among the only attempts at quantifying material properties of embedding media relevant to ultramicrotomy. There appears to be moderate correlation between the measured yield strength and cutting grade of the embedding media from the results. These results were too qualitative to provide enough information about the cutting forces involved in ultrathin sectioning. The testing for this thesis will provide a more quantitative set of data regarding the elastic modulus and stress-strain curves of the embedding media. Furthermore, a detailed and repeatable testing procedure will be established for future testing.

1.3 Background on Cutting Models

In order to eliminate cutting defects, such as chattering, when sectioning such thin layers, a model for this procedure must first be developed. There exist various cutting models that predict material separation for polymer cutting. Through research, there are two main cutting models that may be applicable for ultrathin sectioning of embedded brain tissue.

1.3.1 Williams Model

Williams developed a cutting model for surface layer removal by using a steady state, energy-based analysis approach. The model assumes that the forces and resulting fractures move at the same constant speed. The steady state assumption requires the crack to continue to move in the same direction as well. This model uses an energy balance to account for various cutting regimes based off the removed material: elastic bending, elastic-plastic bending, and plastic shearing. In the elastic bending case, there is no bending energy dissipation of the removed layer. In the elastic-plastic regime, yielding first occurs on the outer layer of the chip and spreads inwards. The center of the core is still elastic and controls the curvature. In plastic shearing, the tool contacts the fracture right behind the chip. There is no bending occurring in this regime. The model also accounts for a special case when the tool tip contacts the crack tip. The four regimes

of behavior for the cutting process identified for this cutting model. The transition between these regimes is based off of a parameter dependent upon yield stress, elastic modulus, fracture toughness, and cutting layer thickness. The four regimes are shown below in Table 1.3. Given relevant mechanical properties of the material and desired cutting dimensions, stable cutting parameters can be determined using this model [9].

Table 1.3: Williams model cutting regimes [9].

Regime transition ratio $\left(\frac{\sigma_Y^2 h}{2EG_C}\right)$	Tool angle (θ)	Cutting regime
> 3	all	elastic
0-3	$\leq 50^\circ$	elastic plastic leading to chip curling, no shearing
	$50^\circ - 90^\circ$	plastic shearing at $h < G_C/\sigma_Y$, otherwise elastic plastic
1-3	$> 90^\circ$	elastic plastic bending
0-1	$> 90^\circ$	plastic shearing for $h < \frac{2G_C}{e_Y\sigma_Y}$, otherwise elastic plastic

1.3.2 Wyeth-Atkins Model

The Wyeth-Atkins model interprets the material separation at the tool edge during polymer cutting using fracture mechanics. The cutting model is based off the testing of cutting the following polymers: PMMA, LLDPE, and Nylon 66. In this model, the relevant length scale is given by $ER/\tau_y^2 = (K_C/\tau_y)^2$, which requires the values for the elastic modulus (E), fracture toughness (R), shear yield strength (τ_y), and critical stress intensity factor (K_C) of the material. All experiments that this model was based off are of orthogonal cutting, permitting two dimensional analyses. This model has two main cases: ductile and brittle cutting. In the brittle cutting case, the cracks rum from the tip of the tool and divert to free space, forming a scalloped surface. The cutting forces fluctuate markedly as the load builds up and the crack propagates. After crack propagation, the load drops and remains at zero until the tool catches up with the new surface and the process repeats. In this regime, there are both Mode I and Mode II displacements.

The more stable case is the ductile cutting regime. Steady load traces are exhibited, producing steady, continuous ductile chips [10].

For many polymers, changing the cutting depth causes the cutting regime to change. There is a critical depth above which brittle chips will form for each polymer. Cutting experimental data shows that measured fracture toughness R_{cut} varies more or less with the tool rake angle. There is a systematic variation in the data suggesting that R_{cut} can be decomposed into separate R_I (tensile) and R_{II} (shear) values in mixed mode ductile chip formation. Negative and small positive rake angles (α) will result in R_{cut} close to R_{II} , while large positive rake angles will result in R_{cut} close to R_I ; if $R_{II} > R_I$, R_{cut} decreases with rake angle, and if $R_{II} < R_I$, R_{cut} increases with rake angle. The ability to decouple these toughness values from steady-state cutting tests can be extremely useful when attempting to model and isolate causes of specific cutting defects [10].

1.4 Thesis Structure

This thesis is separated into several sections, outlining the major parts of the work in this thesis. The theory and calculations behind determining the various material properties gained from this thesis are discussed in Chapter 2. Experimental design and procedure is described in Chapter 3. The steps and considerations in the design and fabrication of a test specimen mold are discussed in detail. Specimen molding and testing procedures are also outlined in this chapter. Results of the tensile testing are presented and analyzed in Chapter 4. The implications of these results and conclusions are discussed in Chapter 5. Further work and testing is also suggested in the last chapter.

MATERIAL PROPERTY CALCULATIONS

The work in this thesis was conducted to determine various important material properties of tissue embedding epoxies that are required for cutting models mentioned in Chapter 1. This thesis is about tensile testing and the material properties that may be calculated from data collected during these tests: elastic modulus, percent elongation at yield and break, nominal strain at break, and ultimate tensile strength. The specifications for the tensile tests will be performed according to the ASTM D638 Standard Test Method for Tensile Properties of Plastics [11]. This standard also recommends calculation methods for these material properties as well. These methods will be described in the subsections below.

2.1 Elastic Modulus

The tensile tests will be performed on an Instron 1125, which will apply and measure a tension force on the installed specimen. An extensometer 3542-100-100-ST will be attached at the gage length segment of the specimen and will output the elongation of this section. The elastic modulus is found by fitting a straight line to the initial linear portion of the elastic region of the stress-strain curve and dividing the difference in stress on the segment of this straight line by the difference in strain, or finding the slope of the line [11]. The straight line will be fitted to the data points in the linear regime by finding a least squares fit using MATLAB. The testing equipment cannot directly measure and output stress values, but they can be calculated using the given geometry of the specimens and the force-displacement data. The strain will be directly measured using an extensometer.

In this test, there is essentially a straight rod—the gage length segment of the specimen—subjected to a tension force applied by the grips on the Instron. This tension force will cause

uniaxial normal stress on the part. In this setup, the system can be assumed to be in equilibrium and the uniaxial normal stress, σ , can be described by Equation (2.1) below.

$$\sigma = \frac{F}{A}, \quad (2.1)$$

where F is the applied tension force, and A is the cross-sectional area. This cross-sectional area will be calculated by multiplying the measured width and thickness of the specimens at the center and within 5 mm of the end of each gage length. These areas will then be averaged to calculate the stress. The gage length of the specimen is significantly longer than the width and depth dimensions, therefore the tensile stress can be assumed to be uniformly distributed across the entire cross-section. The cross-sectional area used to calculate the tensile stress for the stress-strain curves is the average original cross-sectional area along the gage length segment of the test specimen.

2.2 Ultimate Tensile Strength

The ultimate tensile strength of a material can be calculated by dividing the maximum load, F_{max} , by the average original cross-sectional area, A , as shown in Equation (2.2).

$$UTS = \frac{F_{max}}{A} \quad (2.2)$$

This area will be calculated in the same way as explained above for the elastic modulus. In ductile materials, the material will start to undergo plastic deformation and a period of strain hardening. The tensile stress will continue to increase with increasing strain, and cross-sectional area will begin to neck, decreasing the cross-sectional area of the specimen. At some point, the necking will become substantial and cause a reversal of the engineering stress-strain curve, where the stress will appear to decrease as engineering strain increases. This is because the engineering stress is calculated using the original cross-sectional area of the specimen before necking. The highest point of this reversal is the ultimate tensile strength. In brittle materials, there will be little to no plastic deformation before material failure. In this case, the ultimate tensile strength is equal to the stress at the point of failure.

2.3 Yield Strength

Yield strength is the stress at which a material begins to plastically deform. To calculate yield strength, the stress-strain curve will be closely inspected. In many materials, there is no

obvious point at which the material begins to plastically deform. In situations like these, the yield strength is determined by offsetting the linear elastic portion of the stress-strain curve by 0.2% of the strain and finding the intersection of the offset line with the original curve.

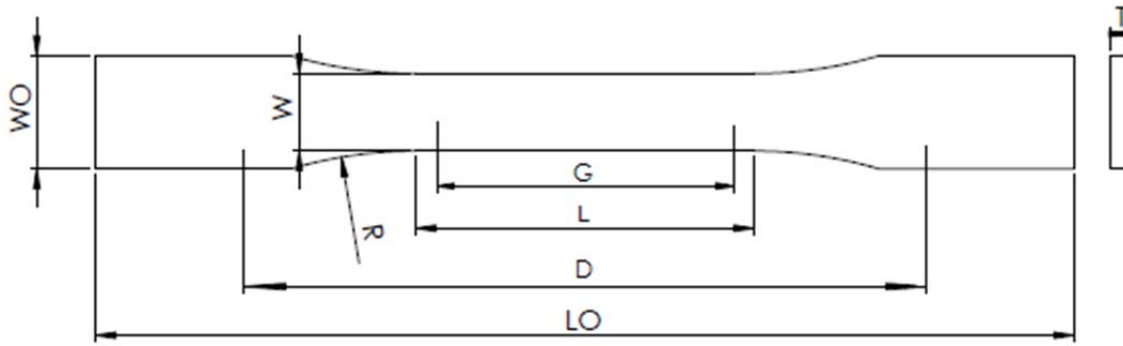
EXPERIMENTAL DESIGN

3.1 Test Overview

In order to understand the cutting forces involved at the nanoscale for the embedding material, it is necessary to first understand the material properties of the material, the most fundamental of which is the elastic modulus. There are several different cutting models that may be applicable, but the elastic modulus a key parameter for all of these models.

The elastic modulus of the embedding medium will vary greatly depending on the ratio of the hardener and accelerator, which will in turn affect the cutting quality. There are many different ratios that the compounds can be mixed. A medium hardness suggested by the manufacturer was used in the tests for this thesis. In the future, it could be possible to test various hardness levels in order to find the optimal level for sectioning.

To find the elastic modulus, tensile tests were performed according to the ASTM D638 Standard Test Method for Tensile Properties of Plastics. The tensile tests were performed on an Instron 1125 universal testing machine with an Epsilon Model 3542-100-100-ST extensometer. The test specimens for the tensile tests were molded according to the dimensions listed in the ASTM D38 Standard, as shown in Figure 3.1.



Variable	Description	Dimension (mm)
W	Width of narrow section	13 ± 0.5
L	Length of narrow section	57 ± 0.5
WO	Width overall, min	$19 + 6.4$
LO	Length overall, min	165 (no max)
G	Gage length	50 ± 0.25
D	Distance between grips	115 ± 5
R	Radius of fillet	76 ± 1
T	Thickness	3.2 ± 0.4

Figure 3.1: Tensile test specimen diagram and dimensions [11].

According to the ASTM standard, at least five specimens for each sample need to be tested to provide enough data for a complete set. These specimens can either be molded or machined. After consideration, the molding method was deemed more efficient for producing specimen, especially for future testing.

3.2 Mold Design

The design of the mold initiates with the goal of producing several tensile testing specimens with the dimensions specified in the testing standard. There are some basic functional requirements for the mold based on the required dimensions for the specimens. The ASTM testing standard suggests that at least five specimens for each sample for isotropic materials must be tested to assure significant data [11]. For this reason, the mold for these specimens should be able to produce five specimens at a time, allowing one full set of specimens for each batch of the epoxy mixture. The molding process should be able to produce full and reliable specimens each time. Having visibly clear material for the sides of the mold would allow for a visible check for air bubbles and partial filling. Furthermore, the volume of epoxy injected into each mold cavity

should exceed the total volume of the cavity. The ASTM testing standard suggests that specimens can be molded or machined, indicating that the surface finish of the specimens should be at least as good as that of machining (6.3-0.8 RA).


The epoxy resin mixture must be cured in the mold in an oven at 60°C for 24 hours. The mold materials must also be able to withstand the same temperature over this amount of time without deformation. To allow for de-molding, the mold will have at least two parts, requiring a clamping mechanism to keep the parts together. This clamping mechanism must be able to overcome the separation force due to the pressure of the fluid inside the mold. Most importantly, the mold must be able to repeatedly and reliably produce testing samples that are within tolerance of the required dimensions according to the standard. The dimensions of the mold should also account for epoxy shrinkage and machine tolerances.

Table 3.1 shows the list of the basic functional requirements for the mold along with the implementation method.

Table 3.1: Mold functional requirements.

Mold Property	Requirement
# of specimens	5
Visibility	Optically clear
Mold filling	Vol epoxy > vol cavity
Surface finish	6.3-0.8 μm RA
Temperature	Maintain structural integrity at 60°C for 24hr
Clamping	$F_{\text{clamping}} > F_{\text{separation}}$

Following these functional requirements, three main mold design methods were considered: one, two and three-part molds. Basic concept drawings of these mold designs are shown in Figure 3.2.



	One-part	Two-part	Three-part
Specimen Quality	O	+	+
Ease of De-molding	O	O	+
Fabrication Time	O	-	-

Figure 3.2: Mold design concept comparison.

Ultimately, a three-part mold design was chosen, because it allowed for the best quality of specimens and easiest de-molding process. While the three-part mold may require some extra time due to the increased number of parts, two of the parts are very simple, so the benefits of the three-part mold outweighs the disadvantages of this design.

The next step in the design process was to consider the mold material that should be used. The materials considered were molded silicone rubber, 3D-printed plastic, or machined aluminum. While silicone rubber would make de-molding very easy, the making of the silicone rubber mold would require an additional mold. While this option is definitely worth exploring in the future, this method would be much more difficult to administer. 3D-printing the mold was another option, but the materials for the 3D printer at hand could not withstand the required curing temperature of the epoxy. In the end, the machined aluminum centerpiece design was chosen.

After various molding tests with the epoxy, it was determined that the epoxy resin binds strongly to glass and acrylic, even with mold release. However, the epoxy separates easily from aluminum. In the final version of the mold, two thin sheets of aluminum shim stock were used on either side of the centerpiece. This allows the specimens to de-mold easily. Five holes were

punched on one of the thin aluminum sheets in order to create a window, allowing for a visual verification of complete mold filling. A 0.635cm (0.25in) sheet of white ABS and 0.635cm (0.25in) sheet of transparent polycarbonate were clamped on the very outside to prevent deflection of the shim stock. The polycarbonate was to be clamped on the side of the mold with the windows in the aluminum shim stock. Other materials can easily be used for these outside sheets, as long as they provide sufficient stiffness, and one side is transparent, allowing visibility. The CAD model of the assembled mold is shown below in Figure 3.3.

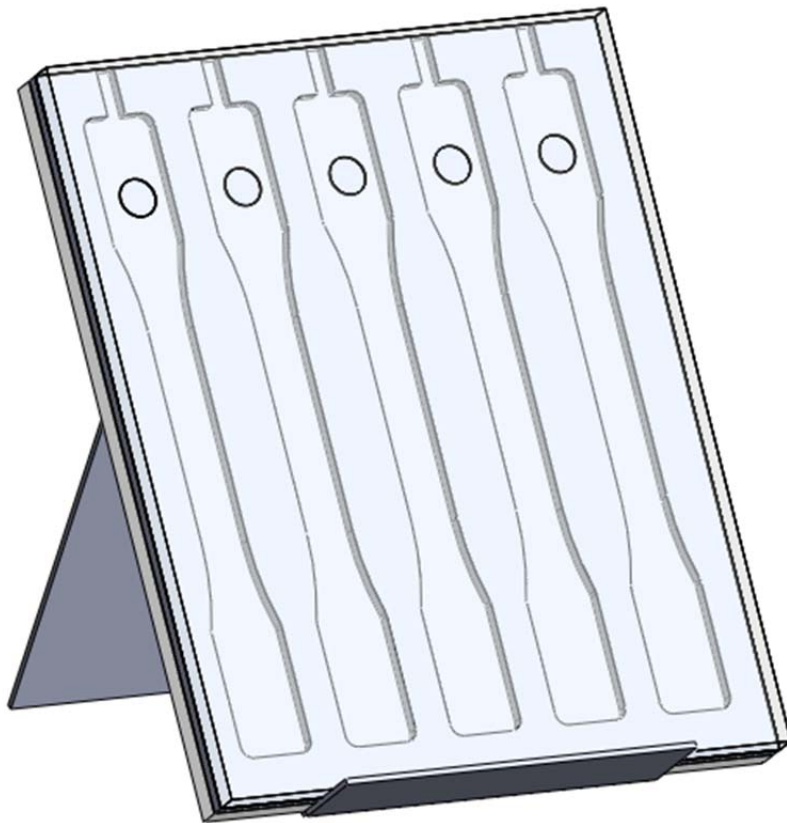


Figure 3.3: CAD model of the assembled mold.

For each of the five specimen cavities, there will be a sprue on the top for epoxy injection. The epoxy will be injected using a Luer lock 14 gage syringe with a 0.211cm (0.083in) outer diameter. The sprues for the molds were designed to be 0.508cm (0.2in) wide to allow ample room for air to escape while filling the molds.

Some basic fluid calculations were performed to determine the separation force and deflection of the mold parts to confirm that the mold design and clamping method will produce satisfactory specimens. The separation force of the mold is a result of the hydrostatic pressure of the fluid within the cavities. The hydrostatic pressure, P , can be described by the expression below.

$$P = \rho gh, \quad (3.1)$$

where ρ is the density of the fluid, g is the acceleration due to gravity, and h is the height of the fluid. A separation force, F , can be calculated by relating the hydrostatic pressure P and total surface area, A in Equation (3.2).

$$F = P \times A, \quad (3.2)$$

The separation force is not constant along the whole plate, but for the purpose of this design, it is only necessary to get a general idea of the average and maximum separation force. The average and maximum separation force for this mold was calculated to be 23.0N and 46.1N respectively. These calculations can be found in Appendix A.2. This separation force is easily overcome using standard clamps along the perimeter of the mold.

Before the mold design could be finalized, a deflection calculation was also performed to ensure that the fluid would not cause significant deflection, causing separation, in the center of the borosilicate. An approximation was made using the beam deflection equation below by assuming the average separation force as a point force applied at the center of the plate.

$$\delta = \frac{Fl^3}{48EI}, \quad (3.3)$$

where δ is the deflection of the beam, F is the applied force, l is the length of the beam, E is the elastic modulus of the beam material, and I is the bending moment of inertia of the beam. Since the relevant cross-section of the beam is rectangular, the bending moment of inertia, I , can be described by the expression below.

$$I = \frac{bh^3}{12}, \quad (3.4)$$

where b is the width of the beam and h is the height of the beam. The maximum deflection of the glass from the separation force was estimated to be 42 μ m (see Appendix A.2.2). This deflection is about 10% of the allowed tolerance for the specimen dimensions, and the thickness variation will remain within tolerance.

3.2.1 Mold Fabrication

The aluminum stock was fly cut on both sides on a mill to ensure flatness and a good surface finish to interface with the glass plates to prevent unnecessary flash and defects. The rough outline of the specimens and sprues then cut out using a water jet. The part was then lined up in a CNC mill to machine for a smooth surface finish on the inside walls. The small air-channels were also milled on both sides of the aluminum part. The borosilicate pieces were cut down to the right size, but otherwise not machined. The mold stand was made by bending a sheet of aluminum stock.

3.3 Specimen Preparation

The specimen preparation procedure was based off of the data sheet from Electron Microscopy Sciences (EMS), the manufacturer of EMBed-812. This epoxy contains four different chemicals that are mixed together at a given ratio to produce the final embedding epoxy resin: EMBed-812 resin, specially distilled Dodecenyl Succinic Anhydride (DDSA), Methyl-5-Norbornene-2,3,-Dicarboxylic Anhydride (NMA), and an accelerator DMP-30. Since the specimens used for the thesis do not contain fixed tissue samples, the procedures for fixation and dehydration of the tissue can be disregarded. The mixing instructions for the epoxy resin suggest two different methods: a two-part mixture method, and a single-step mixing formula. The manufacturer did not indicate any distinction between the two methods, so the simplest method—the single step formula—was chosen. The manufacturer also suggests three different formulations depending on the desired hardness of the block. For this thesis, a medium hardness was chosen. The amounts of each of the compounds were scaled up using the same proportions to produce enough total epoxy to fill the mold cavities. For future tests, it may be advantageous to test other levels of hardness to compare the elastic moduli and cutting qualities [12]. The formulations used for mixing can be found below in Table 3.2.

The EMBed-812 resin and anhydrides (DDSA and NMA) were heated to 60°C on a hot plate prior to mixing in order to reduce the viscosity, as recommended by the manufacturer. These compounds were then measured out using a graduated cylinder. The amount of DMP-30 was measured using a pipet instead of a graduated cylinder, because the amount of DMP was much smaller and needed to be much more precise than any of the other compounds. The actual amounts used in each mixture batch of specimens can be found in Table B.1 in Appendix B.1.

Table 3.2: EMBed-812 mixing ratios.

Compound	Recommended Vol (ml)
EMBed-812	49.1
DDSA	39.3
NMA	19.7
DMP-30	1.89

These compounds were then all poured into a beaker together and mixed thoroughly using a stirring rod. Once the compounds were uniformly stirred, the mixture was placed in a miniature vacuum chamber for 15 minutes to remove air bubbles introduced to the mixture during the mixing process. While the high viscosity of the epoxy resin prevented all of the bubbles from being removed during this process, most of the bubbles were removed. The mixture was then poured into a large syringe with a 14 gauge blunt tip and injected slowly through the sprues into each of the five cavities in the mold. Once the molds were completely filled, the mold was placed carefully on the stand and placed in a Cole-Parmer 05015-58 Laboratory Oven set at 60°C for 24 hours. After 24 hours, the mold was removed from the oven and cooled to room temperature before disassembly and specimens were removed. After demolding and before tensile testing, the relevant dimensions of each specimen was measured and recorded. These measurements can be found in Table B.2 in Appendix B.1. Figure 3.4 shows the epoxy mixing and molding process used in this thesis.

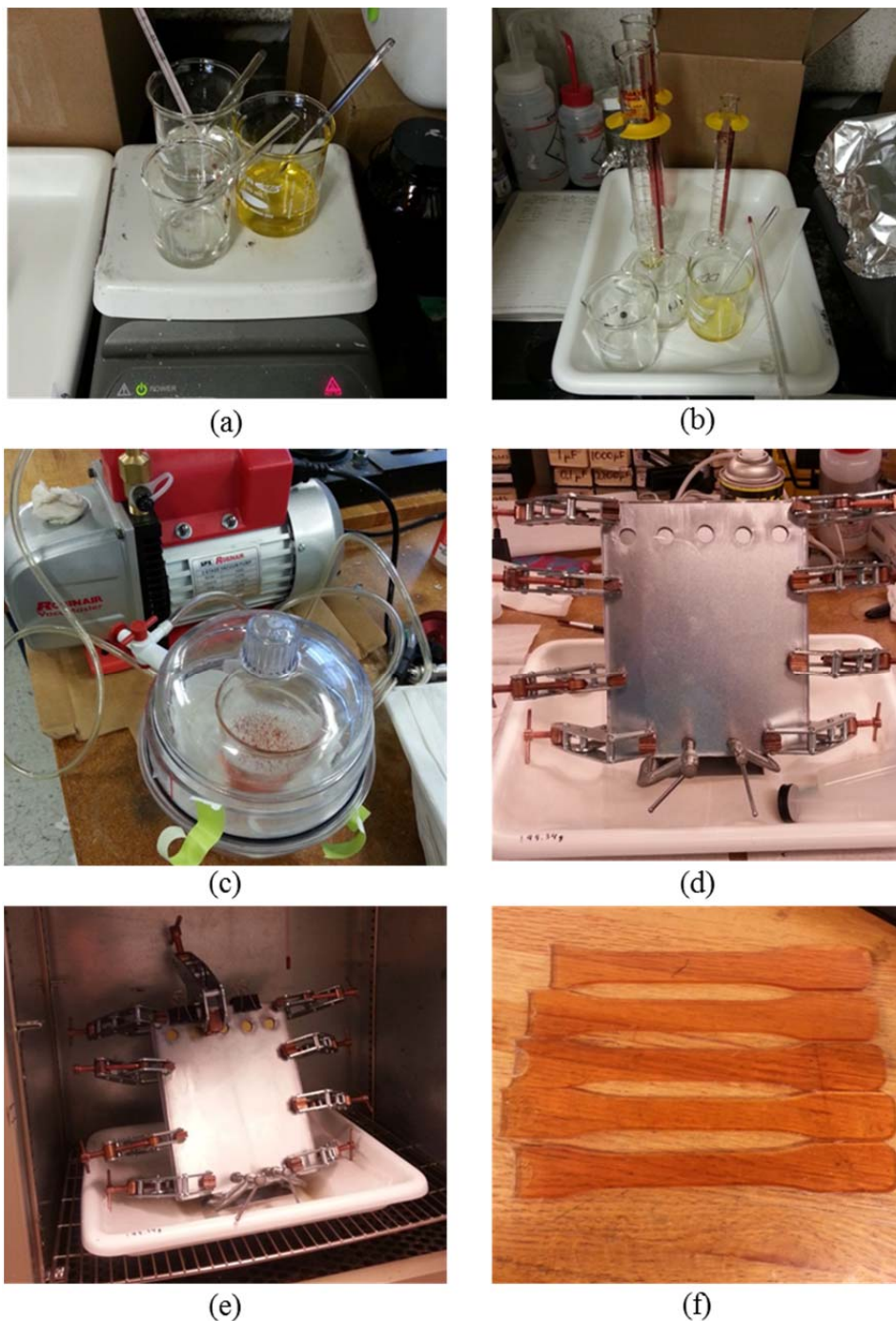


Figure 3.4: Epoxy mixing and specimen preparation procedure.

(a) Chemicals are heated on a hot plate to 60°C before mixing to decrease viscosity. (b) The compounds are measured using graduated cylinders and a pipet and mixed in a beaker. (c) In order to decrease air bubbles, the mixture is degassed in a vacuum chamber. (d) The mold parts are sprayed with mold release and assembled using clamps. (e) The mold is filled and placed in the laboratory oven at 60°C for 24 hours (f) The parts are removed from the mold.

3.4 Experimental Design

The procedures for tensile testing were based off the recommended procedures in the ASTM D638 Standard Test Method for Tensile Properties of Plastics. The specimens were molded following the recommended shape and size in the standard. These specimens will then be clamped in an Instron universal testing machine. An extensometer will be attached to the gage length segment of the specimen to measure strain. The standard recommended a testing speed of 5mm/min; however after some testing, this speed was determined too fast for this material and a speed of 1mm/min was chosen. The test will run until the specimen fractures, and the load, displacement, and stress will be automatically collected by the Instron every half-second. The data will then be post-processed in MATLAB and the relevant material properties calculated. The Instron testing setup is shown below in Figure 3.5.



Figure 3.5: Specimen setup in the Instron with extensometer.

3.5 Sources of Error

There are various sources of error that contribute to the uncertainties of the data collected. The equipment used to measure the data has uncertainties built in. The strain error from the extensometer is reported to be 0.0001 mm/mm. The load cell used is the Instron 2511-305; the loads measured are 0.025% of the maximum load (100 kN). The uncertainties resulting from these measurements are shown in the error bars in the data presented below.

The data used in this test was collected using samples from two mixing batches of epoxy. The exact amounts of each compound in each mixture batch are recorded in Appendix B.1. The material properties of the compound are most sensitive to the DMP-30, which was measured most accurately in both compounds. There should not be a large difference between the two batches, but there are a variety of factors—humidity, temperature—that may possibly account for some of the error. The two batches of specimens were also tested on two different days. The temperature and humidity were both within the required standard range, but the difference may cause the epoxy to behave slightly differently.

4.1 Experimental Results

The Instron machine used for this experiment outputs load and displacement data, and the extensometer directly measures strain. Using this data along with the geometry of each test specimen, a stress-strain curve for each test specimen was plotted and the relevant material properties were calculated using the methods described in Chapter 2. Figure 4.1 shows the measured stress-strain data along with annotations showing how elastic modulus, ultimate tensile strength (UTS), percent elongation at yield, and yield point can be found from the data.

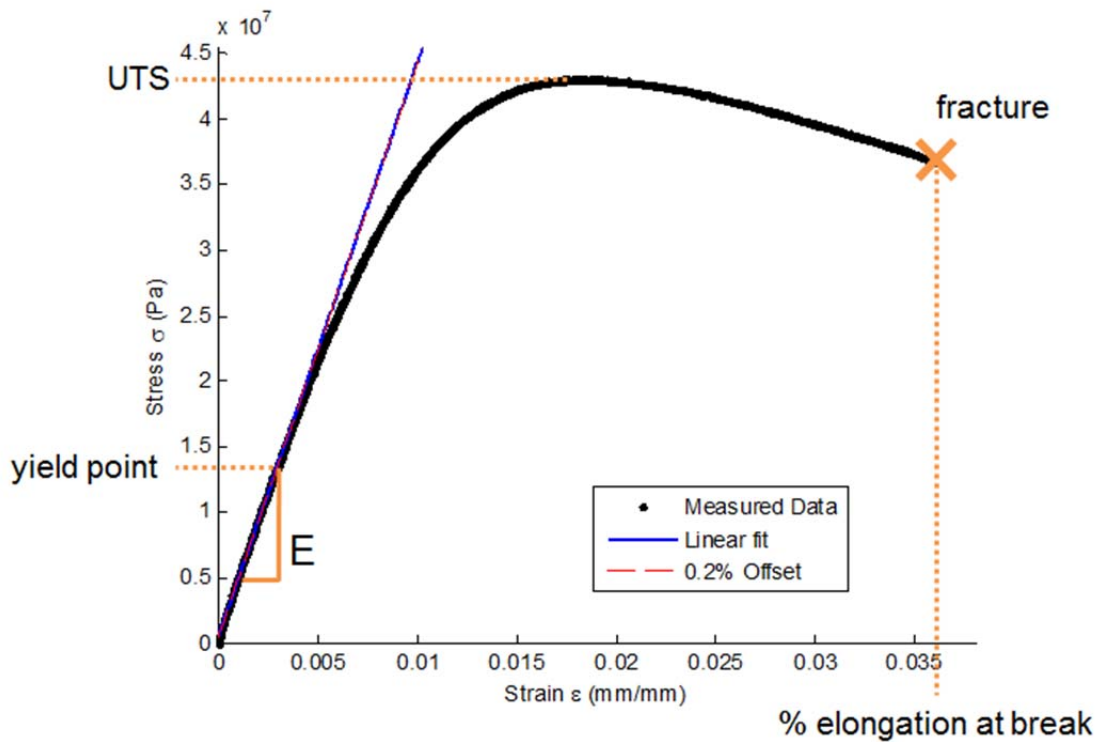


Figure 4.1: Annotated stress-strain curve for Specimen 7.

The calculated material property values along with the uncertainties are displayed in Table 4.1. The material properties for each of the specimens were calculated separately, and an average was determined. The uncertainties were determined by the standard deviation of the eight data points. For the values for each individual specimen, see Table C.1 in Appendix C **Error! Reference source not found.** For the first three specimens (1-3), the extensometer was removed from the sample after entering the plastic regime to prevent extensometer damage. There is no further strain data beyond this point and the percent elongation at breaking was calculated with only the last five samples. For the remaining five samples, the extensometer was left on the sample in order to collect a complete set of data.

Table 4.1: EMBed-812 material property values.

Material Property	Value
Elastic Modulus	4.24 ± 0.27 GPa
Ultimate Tensile Strength	44.8 ± 4.0 MPa
Yield Strength (0.2% offset)	17.2 ± 2.6 MPa
% Elongation at Break	3.73 ± 1.27 %

The stress-strain curves for all eight specimens are plotted below in Figure 4.2.

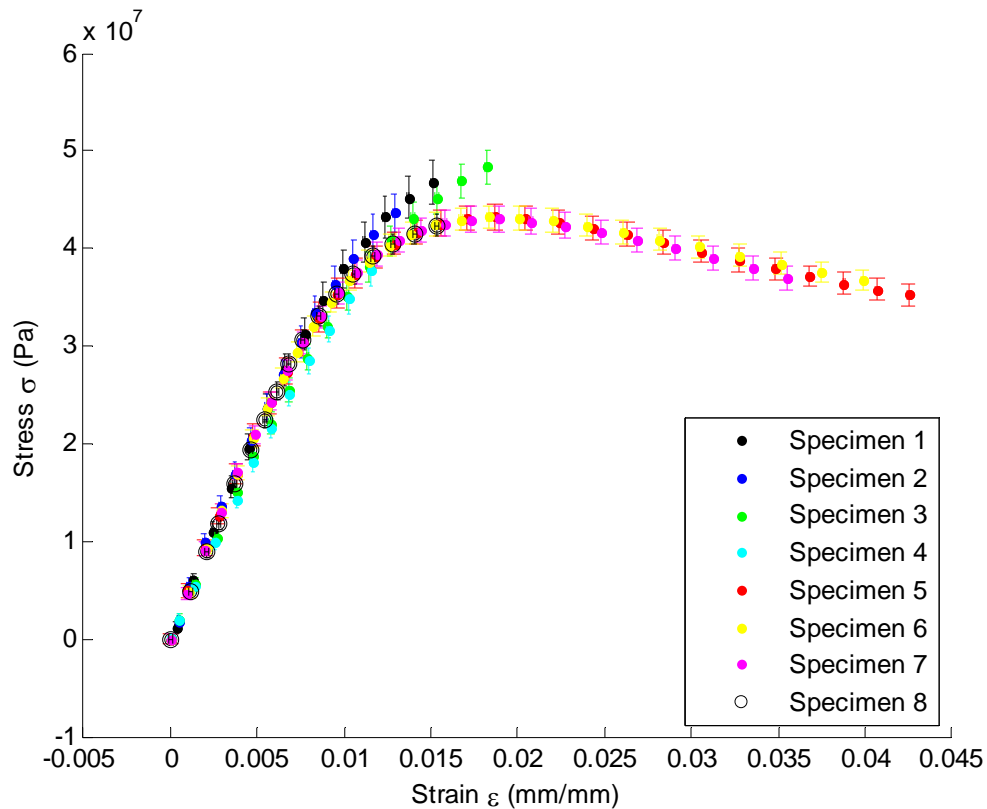


Figure 4.2: Stress-strain curves for all eight test specimens.

The data for specimens 1-3 end early because the extensometer was removed from the sample after entering the plastic regime to prevent extensometer damage.

4.2 Discussion

The data collected in this experimental setup was sufficient to calculate various material properties crucial to determining an accurate cutting model for the nanoscale sectioning of epoxy-embedded tissues. It will be beneficial to perform this test on more specimens to produce

a more complete data set. Acetarin *et al* [8] has previously performed tensile tests on various embedding epoxies, including Epon 812, and determined an elastic modulus of 3.03 GPa. The exact formulations used to prepare the Epon samples were not presented in this paper. According to the manufacturer, the mixing ratios of the DMP-30 will greatly affect the material properties of the cured epoxy resin, but this difference is not quantified. Furthermore, EMBed-812 claims to be a direct replacement for the discontinued Epon 812, but this could also be a cause of the discrepancy between the data collected by Acetarin *et al* [8] and the work in this thesis.

CONCLUSION

The purpose of this research was to understand critical material properties of EMBED-812, a commonly used brain tissue embedding medium. The knowledge of the elastic modulus and ultimate tensile strength play important roles in understanding the cutting forces involved with nanoscale sectioning. The procedures developed in this thesis will help guide further testing for other material properties necessary to develop a full cutting model. The data collected from this work will be used to develop an accurate cutting model and, ultimately, next-generation automated serial sectioning machine. This machine will make it possible to image, layer-by-layer, large volumes of tissue, leading to deeper understandings of neural activity and neurological diseases and disorders.

5.1 Summary

The work presented in this thesis is a first step in understanding the cutting forces and mechanisms involved in nanoscale slicing of embedding epoxy resins and tissue. This research was divided into three main phases: design and fabrication of the mold, specimen preparation, and tensile testing. The parameters for testing were based off the ASTM D638 Standard Test Method for Tensile Properties of Plastics [11]. The desired material properties could be calculated using the testing procedures described in this standard. Once appropriate sample geometry was determined, a three-part mold capable of producing five specimens per molding process was designed and fabricated. The centerpiece of this mold was first cut out of the water jet, and the edges finished in a mill for a good surface finish. The epoxy was mixed using the manufacturer's recommended procedure and mixing ratios; it was then cured in a laboratory oven for 24 hours at 60°C. The specimens were removed from the mold and clamped in an Instron universal testing machine for tensile tests. The test was performed at 1mm/min until

fracture, and the load, displacement, and strain were recorded. The elastic modulus, ultimate tensile strength, offset yield strength and percent elongation at break were calculated from the data collected and averaged across all eight test specimens. The knowledge of these material properties will allow for the development of an accurate cutting model.

5.2 Future Work

While the procedures developed in this thesis produced specimens adequate for testing to collect the intended data, many of the steps in this procedure can be further improved. Further testing can also be performed for more extensive data.

5.2.1 Mold Improvements

The three-part mold used to produce specimens for this research was adequate for short-term testing, but there were various problems that should be addressed for future long-term testing plans. One problem that this mold faced was de-molding. The epoxy resin did not cling to aluminum, but would not release from plastic or glass, even with the use of a mold release. The use of aluminum shim stock made removing the specimens easier, but occasionally, the epoxy would still cling to the plastic through the visibility holes in the shim stock. This problem could be mitigated by switching to a flexible silicone mold. Some of the current existing molds used for producing ultramicrotomy samples are made from silicone, and a similar mold to create tensile testing specimens could also be made.

Another problem that exists with the aluminum mold is leakage. The force provided by the clamps around the perimeter should be sufficient to produce enough clamping force to overcome the separation force in the mold. However, it is possible that the clamps cannot produce a uniform clamping force across the entire mold, so areas that are not directly clamped will show signs of leakage. This problem could also be fixed by using a silicone mold. The silicone material would self-adhere to surfaces and not allow the epoxy fluid to seep through.

5.2.2 Further Materials Testing

The work in this thesis is only the first step in collecting material property data of embedding media. Future work in this area can be in a couple different directions. First of all, only one formulation of EMBED-812 was tested. The manufacturer suggests three levels of

hardness and only the medium one was tested in this work. It is possible that other variations of the hardness will result in slightly different cutting behavior, so other formulations of EMBED-812 should be tested using similar methods to find the optimal embedding recipe. While EMBED-812 is the most commonly used embedding epoxy, there are also a couple others, such as Durcupan and Spurr, which are worth testing. These materials may behave slightly differently when cut at the nanoscale, and one may result in better thin sections than another. The same molding setup can be used to create the testing samples for these tests. For the other epoxy resins, the calculations for separation force, deflection, and air-channel fluid flow must also be re-evaluated for the new fluids.

Testing in this thesis only included tensile tests. Other material properties of the embedding medium, such as fracture toughness and compressive strength, will also be critical in understanding the cutting mechanisms involved when cutting this material at the nanoscale. These other tests will require different molds to produce specimens to meet the standards requirements, but similar mold design strategy and specimen preparation procedures from this thesis can be used for those as well.

Ultimately, the cutting material will be an epoxy-tissue matrix, rather than pure epoxy or tissue. In order to fully understand this matrix, all material testing should also be performed on both embedded tissue in various embedding media as well as pure fixed brain tissue. One can compare the data collected from all three types of media and see how the epoxy-brain matrix differs from both brain tissue and pure epoxy. For these tests, however, there must be some changes made in the specimen preparation steps, as there is no way to cast brain tissue from a mold.

REFERENCES

- [1] W. Villiger and A. Bremer, "Ultramicrotomy of biological objects: from the beginning to the present," *Journal of structural biology*, vol. 104, pp. 178-188, 1990.
- [2] H. K. Hagler, "Ultramicrotomy for biological electron microscopy," in *Electron Microscopy*, ed: Springer, 2007, pp. 67-96.
- [3] "Leica EM UC7: High Quality Ultramicrotome for Precise Room TEMperature and Cryo Sectioning," ed. Vienna, Austria: Leica Mikrosysteme GmbH, 2013, p. 4.
- [4] M. Reck, "Case Study for an Automated Lathe Ultramicrotome," *ASPE Proceedings*, 2010.
- [5] K. Hayworth, N. Kasthuri, R. Schalek, and J. Lichtman, "Automating the Collection of Ultrathin Serial Sections for Large Volume TEM Reconstructions," *Microscopy and Microanalysis*, vol. 12, pp. 86-87, 2006.
- [6] K. J. Hayworth, N. Kasthuri, E. Hartweg, and J. Lichtman, "Automating the collection of ultrathin brain sections for electron microscopic volume imaging," *SfN Poster# 534.6/III27 Abstr*, 2007.
- [7] W. Denk and H. Horstmann, "Serial Block-Face Scanning Electron Microscopy to Reconstruct Three-Dimensional Tissue Nanostructure," *PLoS Biol*, vol. 2, p. e329, 2004.
- [8] J. D. Acetarin, E. Carlemalm, E. Kellenberger, and W. Villiger, "Correlation of some mechanical properties of embedding resins with their behaviour in microtomy," *Journal of electron microscopy technique*, vol. 6, pp. 63-79, 1987.
- [9] J. Williams, "The fracture mechanics of surface layer removal," *International journal of fracture*, vol. 170, pp. 37-48, 2011.
- [10] D. Wyeth and A. Atkins, "Mixed mode fracture toughness as a separation parameter when cutting polymers," *Engineering Fracture Mechanics*, vol. 76, pp. 2690-2697, 2009.
- [11] "ASTM D638: Standard Test Method for Tensile Properties of Plastics," ed. West Conshohocken, PA: www.astm.org, 2010.
- [12] (2014). *EMBed 812 Kit Technical Data Sheet*.

A

MOLD DESIGN AND FABRICATION

Appendix A contains information describing various parts of the design and fabrication process relevant to the mold, including important CAD models, drawings, and calculations.

A.1 Mold CAD Drawings

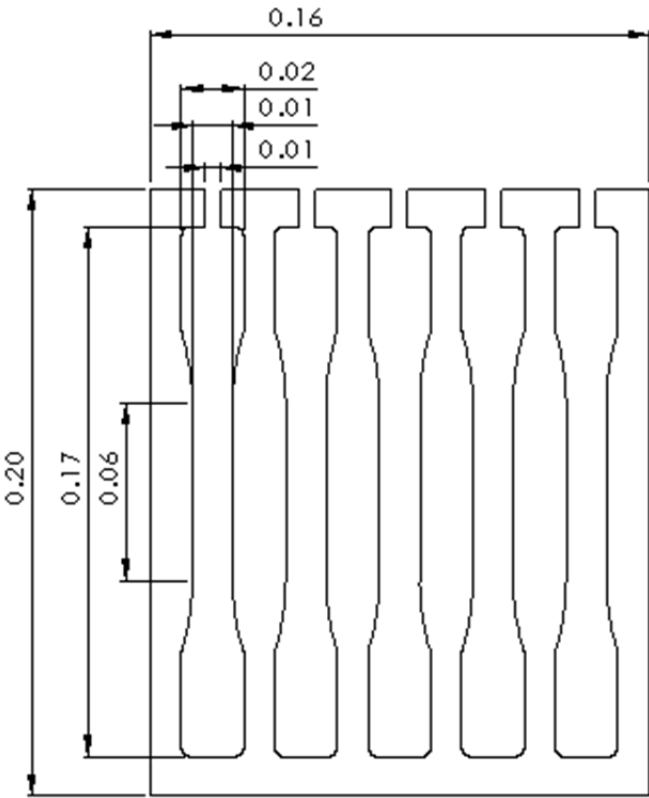


Figure A.1: Dimensioned drawing of mold centerpiece.

A.2 Calculations

This section of the appendix contains all relevant calculations that were done in designing the mold including separation force, and deflection calculations.

A.2.1 Separation Force Calculations

Figure A.2 and Figure A.3 show the calculations performed to compute the maximum and average separation forces for the mold.

$h := 170\text{mm}$	vertical height of cavity
$\rho := 1000 \frac{\text{kg}}{\text{m}^3}$	approximate density of epoxy
$a_g := 9.8 \frac{\text{m}}{\text{s}^2}$	acceleration due to gravity
$P := \rho \cdot a_g \cdot h = 1.666 \times 10^3 \text{ Pa}$	hydrostatic pressure
$A_{\text{cav}} := 27.66\text{cm}^2$	area of single cavity
$F_{\text{cav}} := P \cdot A_{\text{cav}} = 4.608 \text{ N}$	force for single side of single cavity
$n := 5$	number of cavities per mold
$F_{\text{max_separation}} := n F_{\text{cav}} \cdot 2 = 46.082 \text{ N}$	total maximum separation force

Figure A.2: Maximum separation force calculations.

$h := 85\text{mm}$	vertical height of cavity
$\rho := 1000 \frac{\text{kg}}{\text{m}^3}$	approximate density of epoxy
$a_g := 9.8 \frac{\text{m}}{\text{s}^2}$	acceleration due to gravity
$P := \rho \cdot a_g \cdot h = 833 \text{ Pa}$	hydrostatic pressure
$A_{\text{cav}} := 27.66\text{cm}^2$	area of single cavity
$F_{\text{cav}} := P \cdot A_{\text{cav}} = 2.304 \text{ N}$	force for single side of single cavity
$n := 5$	number of cavities per mold
$F_{\text{avg_separation}} := n F_{\text{cav}} = 23.041 \text{ N}$	total average separation force

Figure A.3: Average separation force calculations.

A.2.2 Deflection Calculations

Figure A.4 below shows the deflection calculations for the glass plates due to hydrostatic pressure of the fluid epoxy inside the mold.

$w := F_{\text{avg_separation}}$	total average separation force
$l_{\text{beam}} := 0.2\text{m}$	length of the beam
$E_{\text{polycarb}} := 2.6\text{GPa}$	elastic modulus of polycarbonate
$b := 20\text{cm}$	width of the polycarbonate plate being bent
$h_{\text{polycarb}} := 0.25\text{in}$	thickness of polycarbonate plate
$I := \frac{(b \cdot h_{\text{polycarb}}^3)}{12} = 4.267 \times 10^{-9} \text{ m}^4$	bending moment of inertia of polycarbonate plate
$\delta_{\text{glass}} := \frac{w \cdot l_{\text{beam}}^3}{48 E_{\text{polycarb}} \cdot I} = 346.101 \cdot \mu\text{m}$	deflection of outside polycarbonate sheets

Figure A.4: Mold deflection calculations.

A.3 Mold Centerpiece Process Plans

The process plan for the fabrication of the mold centerpiece is shown below in Figure A.5.

Process Plan	Version: V1, actual	Part name: Mold Centerpiece		Date: 04/19/2014
Step	Task & questions	Machine	Tooling	Measurement
01	Place fixture plate in mill and fly cut it to make square and flat.	CNC Mill	Fly cutter	-
02	Clean off fixture plate and one side of stock with soap, water, and isopropyl alcohol	-	Water, soap, isopropyl alcohol	-
03	Use double-sided tape and clamps to attach stock to fixture plate	-	Double-sided tape	-
04	Fly cut the plate just enough to ensure a flat and square surface. Move clamps as necessary.	CNC Mill	Fly cutter	-
05	Take plate out using isopropyl alcohol and measure thickness using micrometer	-	Isopropyl alcohol, micrometer	Measure and record thickness.
06	Clean off fixture plate and one side of stock with soap, water, and isopropyl alcohol	-	Water, soap, isopropyl alcohol	-
07	Use double-sided tape and clamps to attach stock to fixture plate (with the machined-side down)	-	Double-sided tape	-
08	Fly cut the plate to 3.2 mm. Move clamps as necessary.	CNC Mill	Fly cutter	3.2mm thickness
09	Take plate out using isopropyl alcohol and measure thickness using micrometer	-	Isopropyl alcohol, micrometer	Measure and confirm thickness (3.2 ± 0.4mm)
10	Load blank material onto water jet deck. Weigh down, and zero head. Initiate cutting path from file.	Water jet	-	.dxf file
11	Remove part from water jet, deburr and measure	-	Deburring tool, files, calipers	Confirm general dimensions
12	Use a square to check corners, and mark best corner to line up in mill	-	Square	Square up edge
13	Square up one x and y edge on fixture plate	CNC Mill	1/4" endmill	-
14	Clean off fixture plate and one side of stock with soap, water, and isopropyl alcohol	-	Water, soap, isopropyl alcohol	-
15	Use double-sided tape and clamps to attach part to fixture plate, lining up the two square corners	-	Double-sided tape, parallels	-
16	Use 1/8" flat endmill to finish the inside of mold cavities. Move clamps as necessary.	CNC Mill	1/8" flat endmill	CNC G-code
17	Use 1/16" flat endmill to make small channels. Move clamps as necessary.	CNC Mill	1/16" flat endmill	CNC G-code
18	Take plate out using isopropyl alcohol and measure thickness using calipers	-	Isopropyl alcohol, calipers	Measure and confirm cavity width and channel depth

19	Clean off fixture plate and one side of stock with soap, water, and isopropyl alcohol	-	Water, soap, isopropyl alcohol	-
20	Use double-sided tape and clamps to attach part to fixture plate, flipped over from previous configuration, squaring up the edges to the fixture plate.	-	Double-sided tape, parallels	-
21	Use 1/16" flat endmill to make small channels (0.003" depth). Move clamps as necessary.	CNC Mill	1/16" flat endmill	CNC G-code
22	Remove part using isopropyl alcohol. Deburr, measure and confirm dimensions	-	Isopropyl alcohol, deburring tool, file, calipers/micrometer	Measure and confirm dimensions with part.

Figure A.5: Mold centerpiece process plan used for this thesis.

SPECIMEN PRODUCTION

Appendix B contains relevant information pertaining to the specimen production.

B.1 Actual Specimen Mixture Quantities

Table B.1: Actual quantities in epoxy mixtures.

Compound	Recommended Vol (ml)	Batch 1 Actual Vol (ml)	Batch 2 Actual Vol (ml)
EMBed-812	49.1	49.0	49.2
DDSA	39.3	40.0	39.5
NMA	19.7	19.7	19.7
DMP-30	1.89	1.89	1.89

B.2 Actual Specimen Dimensions

Figure B.1 is a labeled schematic of the relevant dimensions of the specimens. The measured dimensions of the molded specimens are shown in Table B.2 below.

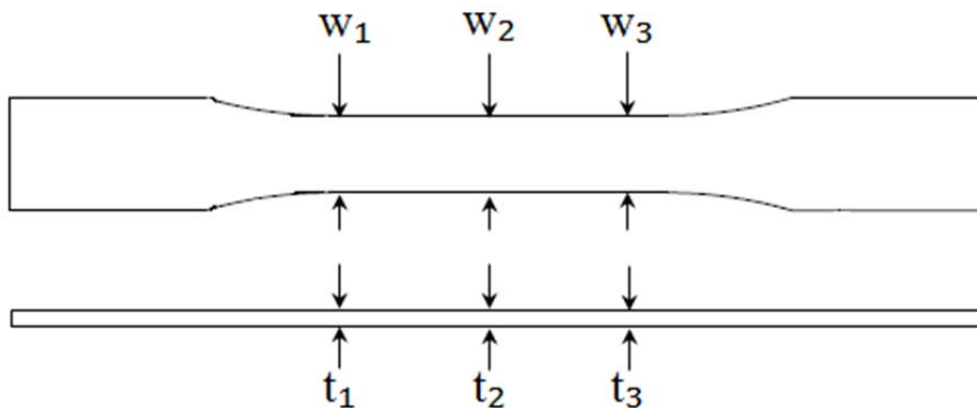


Figure B.1: Labeled schematic of relevant testing specimen dimensions.

Table B.2: Measured dimensions of molded specimens in mm.

Specimen #	w ₁	t ₁	w ₂	t ₂	w ₃	t ₃
1	13.23	3.39	13.25	3.26	13.15	3.48
2	13.09	3.50	13.31	3.36	13.12	3.52
3	13.15	3.43	13.18	3.33	13.11	3.48
4	13.16	3.48	13.06	3.35	13.04	3.47
5	13.17	3.49	13.29	3.50	13.22	3.36
6	13.36	3.54	13.47	3.57	13.44	3.49
7	13.37	3.44	13.41	3.39	13.41	3.50
8	13.32	3.52	13.38	3.56	13.40	3.48

C

INDIVIDUAL SPECIMEN MATERIAL PROPERTY VALUES

Table C.1 contains the calculated and measured values of the material properties of each individual specimen tested.

Table C.1: Material property values for each separate specimen.

Specimen #	Elastic Modulus (GPa)	UTS (MPa)	Yield Strength (MPa)	% Elongation
1	4.48 ± 0.01	48.6 ± 2.3	1.70	-
2	4.41 ± 0.07	48.9 ± 2.1	2.14	-
3	3.92 ± 0.01	50.3 ± 1.8	1.64	-
4	3.73 ± 0.03	38.5 ± 2.3	1.91	4.95
5	4.37 ± 0.03	43.3 ± 1.0	1.49	4.29
6	4.42 ± 0.01	43.3 ± 1.1	1.71	4.16
7	4.38 ± 0.03	43.1 ± 1.2	1.31	3.60
8	4.24 ± 0.01	42.6 ± 1.1	1.86	1.62